**ОРИГИНАЛЬНАЯ СТАТЬЯ**

**Известия вузов России. Радиоэлектроника. 2019. Т. 22, № 4**
**Journal of the Russian Universities. Radioelectronics. 2019, vol. 22, no. 4**

**ORIGINAL ARTICLE**

**Радиолокация и радионавигация**
**Radiolocation and Radio Navigation**

UDC 621.396.6+551.510.535+550.388.2 https://doi.org/10.32603/1993-8985-2019-22-4-53-65

# Correlation between the Orientation of Cross-Field Axes of Small-Scale Anisotropic Irregularities in Midlatitude Ionosphere and Drift Direction in the F Region

***Valery A. Panchenko[1]✉, Viktor A. Telegin[1], Natalia Yu. Romanova [2]***

*[1]Pushkov Institute of Terrestrial Magnetism,*
*Ionosphere and Radio Wave Propagation Russian Academy of Sciences*
*4 Kaluzhskoe Hwy, Moscow 108840, Troitsk, Russia*

*[2]Polar Geophysical Institute*
*15 Khalturina Str., Murmansk 183010, Russia*

✉*panch@izmiran.ru*

**Abstract**

**Introduction.** It has been previously reported that small-scale irregularities (SSI) in the polar ionosphere are elongated along the magnetic field and anisotropic in its cross-field direction. At the same time, the largest of the SSI cross-field axes tends to orient along the SSI drift direction. However, there is no evidence of direct correlations of SSI anisotropy and ionospheric drift directions in the middle latitudes.

**Objective.** A direct comparison of the experimental data of SSI shape with motion parameters of irregularities was measured at the same place (Moscow) at the same time. Previously, experimentally obtained values of SSI cross-field anisotropy orientation in the midlatitude ionosphere were compared only with the neutral winds model.

**Materials and methods.** A tomographic approach was used to determine SSI anisotropy parameters by processing radio scintillation signals during overfly by several navigation satellites emitting on frequencies of 150 MHz and 400 MHz. Estimations were obtained of the ratio between the ellipsoid axes and cross-field anisotropy orientations in the framework of the SSI model in a form of magnetic field-oriented ellipsoids with three different dimensions along and across the Earth's magnetic field. The parameters of irregularities were obtained by selecting model parameters at a time when the calculated logarithm dispersion of the satellite signals relative amplitude during orbit is the closest to the experimentally obtained curve.

Estimations were obtained of the velocity and drift direction of medium-scale irregularities (MSI) by using DPS-4 ionosonde data acquired while decametre-wave radar studies of ionosphere from the Earth's surface. Simultaneous measurements of Doppler frequency shifts and incident angles of scattered waves allowed estimations of three components of the medium-scale irregularities drift velocity to be obtained.

**Results.** There was evidence of a good correlation between the drift direction of medium-scale irregularities and cross-field anisotropy orientation of small-scale irregularities. The difference in the drift directions of MSI and in the orientation of the cross-field axes of SSI varied from 3 to 10 degrees (provided the spatial coincidence of the ionosphere regions where the measurements were carried out).

**Conclusion.** In constructing a model of the radar backscattering signal in the HF band, the correlation between the cross-field anisotropy orientation of the elongated irregularities and their drift direction can be useful when there is a lack of information on ionospheric irregularities.

**Key words:** ionosphere, cross-field anisotropy orientation, irregularities drift, backscattering, over-the-horizon radar

**For citation:** Panchenko V. A., Telegin V. A.,Romanova N. Yu. Correlation between the Orientation of Cross-Field Axes of Small-Scale Anisotropic Irregularities in Midlatitude Ionosphere and Drift Direction in the F Region.Journal of the Russian Universities. Radioelectronics. 2019, vol. 22, no. 4, pp. 53–65. doi: 10.32603/1993-8985-2019-22-4-53-65

**Conflict of interest.** The authors declare no conflict of interest.

Submitted 25.04.2019; accepted 03.06.2019; published online 27.09.2019

**Известия вузов России. Радиоэлектроника. 2019. Т. 22, № 4**
**Journal of the Russian Universities. Radioelectronics. 2019, vol. 22, no. 4**

**ОРИГИНАЛЬНАЯ СТАТЬЯ**

**Радиолокация и радионавигация**
**Radiolocation and Radio Navigation**

**ORIGINAL ARTICLE**

# Связь ориентации поперечных осей мелкомасштабных анизотропных неоднородностей среднеширотной ионосферы с направлением дрейфа на высотах F-области

***В. А. Панченко [1]✉, В. А. Телегин[1], Н. Ю. Романова[2]***

*[1]Институт земного магнетизма, ионосферы и распространения радиоволн им. Н. В. Пушкова РАН*
*Калужское шоссе, д. 4, Москва, г. Троицк, 108840, Россия*

*[2]Полярный геофизический институт*
*ул. Халтурина, д. 15, Мурманск, 183010, Россия*

✉ *panch@izmiran.ru*

**Аннотация**

**Введение.** Ранее было установлено, что в полярной ионосфере мелкомасштабные неоднородности (МН), вытянутые вдоль магнитного поля, анизотропны в поперечном к магнитному полю направлении. При этом бóльшая из поперечных осей МН имеет тенденцию ориентироваться вдоль направления дрейфа МН. Для средних широт прямые сопоставления направления анизотропии МН и направления ионосферного дрейфа отсутствовали.

**Цель работы.** Прямое сопоставление экспериментальных данных о форме МН с параметрами движения неоднородностей при измерениях в одном и том же месте (Москва), в одно и то же время. Ранее экспериментально полученные значения ориентации поперечной анизотропии МН в среднеширотной ионосфере сравнивались только с моделью нейтральных ветров.

**Материалы и методы.** Для определения параметров анизотропии МН использован томографический подход – обработка радиомерцаний сигналов при пролете ряда навигационных спутников, излучающих частоты 150 и 400 МГц. В рамках модели МН в виде ориентированных по магнитному полю эллипсоидов с тремя разными характерными масштабами размеров вдоль и поперек магнитного поля Земли получены оценки соотношения осей эллипсоидов и ориентации поперечных осей анизотропии. Параметры неоднородностей получены подбором параметров модели, при которых расчетный ход дисперсии логарифма относительной амплитуды сигналов спутников по мере их движения по орбите наиболее близок к экспериментально полученной зависимости.
Оценки скорости и направления дрейфа среднемасштабных неоднородностей (СН) получены по данным ионозонда DPS-4, при радиолокации ионосферы декаметровыми волнами с поверхности Земли. Одновременные измерения доплеровских сдвигов частоты и углов прихода на землю рассеянных волн позволяют получить оценки трех компонент скорости дрейфа среднемасштабных неоднородностей.

**Результаты.** Обнаружено хорошее соответствие между направлением дрейфа среднемасштабных неоднородностей и ориентацией поперечной анизотропии мелкомасштабных неоднородностей. Разница в направлениях дрейфа СН и ориентацией поперечных осей МН изменялась от 3 до 10 градусов (при условии пространственного совпадения областей ионосферы, где проводились измерения).

**Заключение.** Обсуждаемая связь ориентации поперечной анизотропии вытянутых неоднородностей и направления их дрейфа может быть полезна в условиях дефицита информации о неоднородной ионосфере при построении модели сигнала обратного рассеяния в задачах радиолокации в КВ-диапазоне.

**Ключевые слова:** ионосфера, ориентация неоднородностей, дрейф неоднородностей, обратное рассеяние, загоризонтная радиолокация

**Для цитирования:** Панченко В. А., Телегин В. А., Романова Н. Ю. Связь ориентации поперечных осей мелкомасштабных анизотропных неоднородностей среднеширотной ионосферы с направлением дрейфа на высотах F-области // Изв. вузов России. Радиоэлектроника. 2019. Т. 22, № 4. С. 53–65. doi: 10.32603/1993-8985-2019-22-4-53-65

**Конфликт интересов.** Авторы заявляют об отсутствии конфликта интересов.

Статья поступила в редакцию 25.04.2019; принята к публикации после рецензирования 03.06.2019; опубликована онлайн 27.09.2019

**Introduction.** All types of remote, non-contact control methods and devices use waves in one or another medium. For example, acoustic waves are used in hydroacoustics and sound direction targeting in artillery systems. Acoustic longitudinal and transverse waves are used to register seismic events in the earth. Electromagnetic waves in the optical range are used for lidar measurements, and electromagnetic waves in the radio range ($10^5$–$10^{12}$ Hz) are used for radar and positioning systems. In all cases, the importance of the information received depends on the correct definition of the wave propagation laws, signal properties, predefined properties of objects, and, last but not least, on the most complete description of the signal propagation medium characteristics. Although these characteristics are different for various media, the common thing is that these parameters determine the refractive index for the waves used. For example, distributions of density and salinity of water and temperature are important in the hydroacoustics, while the medium permittivity distribution is important in electromagnetic sounding.

The interpretation of the results of the measurement of the characteristics of the monitored object characteristics can be improved by the direct measurement of the characteristics of the environment. For example, this can be achieved using additional channels or systems in radars, in order to determine interference due to a signal scattering in its propagation medium or using multifrequency systems in satellite navigation systems. In some cases, these real measurements are ineffective, difficult or impossible. Therefore, it is important to choose a medium model that correctly describes the basic properties of the refractive index. These models are created for each of the media and should include a deterministic part describing the behaviour of the averaged parameters in space and time, as well as their random variability in time and space (medium irregularities).

In this article, the authors have focused on radio wave propagation in the ionosphere. The ionosphere is an electrically conductive medium where its refractive index is determined by an electron density in the weakly ionised plasma. A large amount of phenomenological data has been accumulated and systematised for the ionosphere [1, 2]. Ionosphere regular structure models have been built and they are constantly improving. The models include ionisation distributions depending on regional geographical coordinates, time of year and day, averaged indices of solar activity and current magnetic activity [3, 4] and even lunar tides. Efforts have also been made to build a distribution in space and time of ionospheric irregularities (II) [5, 6] responsible for signal behaviour of communication, positioning and radar systems (fading, shape distortion, time spreading, spectrum distortion of received signals). These properties must be known and considered in issues associated with radar, design and operation of positioning systems (GPS, GLONASS, Galileo, etc.). The reduction in the accuracy of coordinate definition of these systems and even failures during strong ionospheric disturbances are well known [7]. In over-the-horizon radar one of the main sources of interference is backscattering on ionospheric irregularities. Therefore, any phenomenological data and predefined information about ionospheric irregularities is useful in the aims of ensuring the correct design and operation of over-the-horizon radar and communication systems.

The article sets out the parameters of scattering irregularities based on an understanding of the ionosphere as a plane layered medium with refractive index $n$. This is dependent on the height $z$ and radio frequency $\omega$, and adds (immersed) irregularities of various spatial and temporal scales. When sounding takes place from the Earth's surface in the ionosphere without irregularities, then radio waves in the frequency range below a certain critical frequency $\omega 0$ undergo total internal reflection in a region where the refractive index $n(z, \omega)$ is equal to zero due to its decrease with height [2]. The surfaces $n(z, \omega) = 0$ for the plane layered model of the ionosphere without irregularities are parallel to each other. The reflection region when monostatic sounding is performed at a fixed frequency $\omega \le \omega_0$ is unique. The wave returns to the earth vertically from the zenith. The surfaces of equal electron density are no longer parallel to each other when different scale irregularities are added into the plane layered ionosphere (Fig. 1). The condition of the return of the probe wave energy to the radiation point is the local perpendicularity of the beam to the reflecting surface where $n(x, y, z, \omega) = 0$. The reflected radio wave energy arrives not from one point (zenith), but is distributed in a cone of arrival angles due to scattering on irregularities of different spatial and temporal scales.

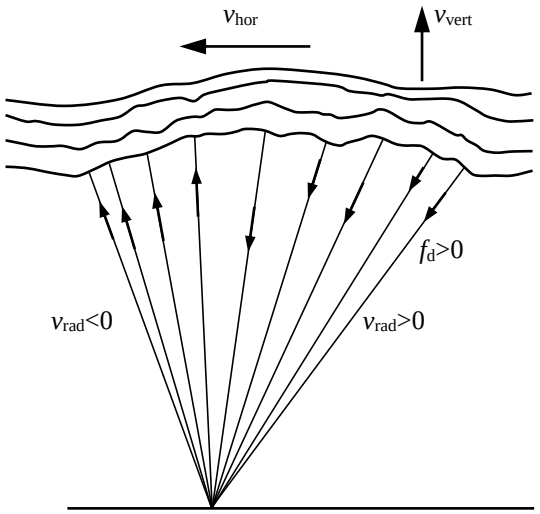


*Fig. 1*. Ionosphere model with different scale irregularities

The shape of the irregularities influences the scattering processes. The so-called travelling ionospheric disturbances with characteristic spatial scales of $10^2 \ldots 10^3$ km possess an arbitrary shape. They are the reason for the quasi-periodic variations of critical frequencies and ionospheric layers F1 and F2 heights with periods from 5 minutes to 2 hours. At the same time, observed backscattered signals indicate the presence of so-called small-scale irregularities (SSI) with scales of $10^{-1} \ldots 10^3$ m [8]. These are strongly elongated along the magnetic field (Fig. 2). The ionosphere model with different scale irregularities is shown schematically in Fig. 1.

Random small-scale irregularities are usually described by a correlation function in a form of an ellipsoid with the major, largest axis oriented along the Earth's magnetic field (Fig. 2, *a*). This elongation is due to the fact that the diffusion coefficients of electrons and ions along and across the magnetic field are very different. Experimental estimates of the ellipsoid axes' ratio (elongation degree) vary greatly from 3–4 [8] to several hundred [9]. It is often noted that small-scale irregularities can be represented as spheroids, but studies over different years show that it is not always reasonable [10, 11]. Thus, further small-scale irregularities are considered transversely anisotropic, so the transverse axes of ellipsoids should not be assumed to be equal (Fig. 2, *b*).

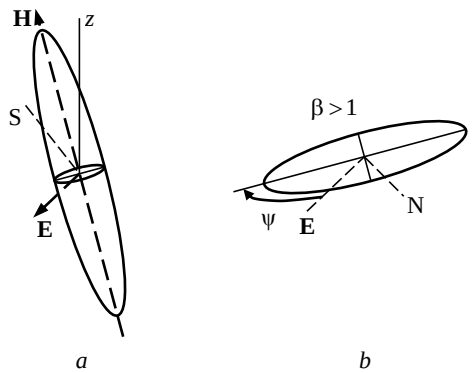


*a* *b*

*Fig. 2*. Correlation function of small-scale inhomogeneities: *a* – correlation function; *b* – cross-section

This objective of the article is a non-trivial comparison of the shape of ionospheric irregularities with their motion parameters, namely, the SSI cross-field anisotropy orientation with the medium-scale irregularities (MSI) drift direction in the F region. These were experimentally measured at the same place (Moscow) at the same time. Small-scale irregularities are considered to be irregularities with dimensions of 0.1…3 km, and medium-scale irregularities are considered as irregularities with dimensions of 5…50 km. It should be noted that principally different methods for measuring the SSI and MSI parameters are used. The SSI shape and orientation are determined by using the tomographic approach [10] by means of receiving low-flying satellites signals from the Earth's surface. MSI drift parameters are measured by sensing the ionosphere from the Earth's surface by using the DPS-4 ionosonde [12–15].

**The tomographic approach** for determining cross-field anisotropy orientation is developed in [10]. It considers the model of randomly arranged small-scale irregularities in a form of ellipsoids elongated along the magnetic field. It is assumed that during measurements, their shape and location are unchanged. Radial trajectories from an artificial satellite (AS) to a terrestrial receiver cross a region with SSI. The logarithm dispersion of the AS signal relative amplitude under the assumption of the weak irregularities and backscattering absence is obtained (including the method of experimental estimation parameter $\chi$) by using Rytov's approximation [16]: $\chi = \ln(A/A_0)$, where $A$ is the fluctuating signal amplitude in the presence of irregularities; $A_0$ is the non-fluctuating signal amplitude in a medium without irregularities. The expression for $\chi$ in [10] includes elongation of the irregularities along the magnetic field $\alpha$; elongation of the irregularities perpendicular to the magnetic field $\beta$ (the ellipsoid largest transverse axis) and angle $\psi$ between this axis and the east (see Fig. 2),

where $\alpha > \beta > 1$. The angle $\psi$ is referred to as the cross-field anisotropy orientation. The anisotropic SSI parameters α, β, and ψ are obtained as a result of AS signals amplitude processing.

The simulation shows [10] that anisotropy parameters significantly affect changes in the logarithm dispersion of the signal relative amplitude $(\chi)$ while satellite passes near the magnetic zenith. On the contrary, the height of a region with irregularities, regional thickness and degree of reduction in the irregularities spatial spectrum do not significantly affect $\chi$. Details of the processing technique for experimental data, additional assumptions about the irregularities parameters and their location are given in [10].

In practice, the following procedure is applied. A terrestrial receiver records a radio signal at a frequency of 150 MHz when a satellite enters a radio visibility zone. The recorded signal is distorted when passing through the F region of the ionosphere with small-scale irregularities. The variance values $\sigma^2(\chi)$ are calculated from the experimental data by using equations from [10] and the satellite position. Increased amplitude fluctuations of the received radio wave can be observed due to the scattering when the "satellite–receiver" beam crosses the region with the SSI. This leads to an increase in variance $\sigma^2(\chi)$ (Fig. 3, line *1*) and formation of the maximum which spatially covers the region with irregularities. It is possible to determine the SSI spatial parameters α, β, and ψ, if the value at the maximum is several times higher than the background level. To this end, an experimental dependence approximation (Fig. 3, line *2*)

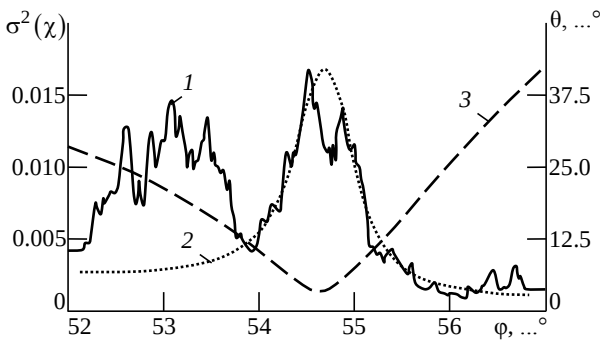


*Fig. 3*. The dependence between the logarithm dispersion of signal relative amplitude and angle between the magnetic field vector and line connecting the satellite with its latitude (Moscow, 11.01.2014 00:25 UT):
*1* – experiment; *2* – simulation; *3* – angle between the magnetic field vector and line connecting the satellite with its latitude

needs to be constructed according to the equations from [10]. The approximation is calculated by selecting the α, β, and ψ numerical values. As shown in [10] the width of the theoretical maximum depends mainly on the α and β values. The spatial position of the theoretical maximum significantly depends on the ψ value and in most cases is determined with an accuracy of 2…3 °.

The measurements presented in this article were performed in Moscow. The angle between the direction line towards zenith and magnetic field vector is 14 °.

The satellite trajectory and maps are usually given in geographical coordinates. Thus, the angle ψ in magnetic coordinates is replaced by the angle $\psi_a$, obtained by projecting the ψ direction onto the horizontal plane. However, unlike [10], this angle is measured in a standard way, namely clockwise from a direction to the geographical north.

The method for determining the parameters α, β, and $\psi_a$ can be demonstrated by using the example shown in Fig. 3 (φ is the satellite geographic latitude). In this case, the angle θ between the magnetic field vector and direction line towards the satellite initially decreases from 31º to 3.5º, and then increases up to 44.9º (Fig. 3, line 3). At the same time, a peak with a width of about 1º near the magnetic zenith $(\theta_{\min} = 3.5^\circ)$ in the $\sigma^2(\chi)$ graph (line 1) is formed. Simulation (line 2) shows that the best agreement is obtained when $\alpha = 9$, $\beta = 2$, $\psi_a = 95^\circ$. It should be noted that the approximation of SSI in the form of spheroids $(\beta = 1)$ is unsatisfactory.

**Radar method for medium-scale irregularities drift estimation.** From the hardware point of view, the DPS-4 ionosonde located in Moscow (ISMIRAN) [12] is a pulse-Doppler radar which uses convolutions of code-phase-shift keying (CPSK) sequences. It has a phased receiving low-element antenna array. The ionosonde operates at a variable frequency in the range of 1…40 MHz. Details of DPS-4 operation and methods of ionogram processing can be found in [12, 13, 15]. Only the features of this apparatus most significant for heterogeneous structure studying are noted further. The plane polarised wave emitted by the antenna divides into two elliptically polarised waves due to the Earth's magnetic field presence when probing the ionosphere. These are the so-called ordinary wave (O-wave) and extraordinary

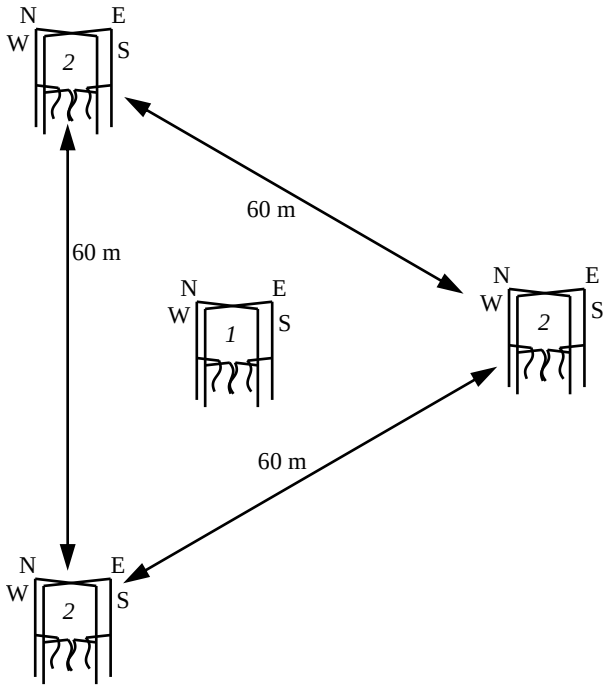


*Fig. 4*. The antenna system of the DPS-4 ionosonde

wave (X-wave). They have different refractive indices and are reflected at different ionosphere heights. Typically, ionosonde terrestrial antennas receive a superposition of O- and X-waves. The reception of radio waves of only one of two polarisations (usually O-wave) needs to be ensured when analysing the field of radio waves received on earth, in order to determine the characteristics of scattering irregularities. In DPS-4 this issue is solved by using crossed frames in combination with polarisation switches as receiving antennas (Fig. 4, *2*). The magnetic field in the ionosphere above Moscow is deviated from the vertical on 13…14°, and O- and X-waves are polarised almost circularly. It is therefore, sufficient to sum the frames signals when one of them is previously shifted at ±90° in phase, in order to suppress undesirable polarisation in each antenna. The circular polarisation antenna (Fig. 4, *1*) is also used for transmission to improve the undesirable polarisation suppression in DPS-4 [12]. In this case, each of antenna crossed sheets receives a signal from the corresponding transmitter, and these signals are phase shifted relative to each other at ±90°.

The main operation mode of the DPS-4 is to record ionograms (Fig. 5), i.e. the measurement of the dependence of the signal delay reflected from the ionosphere (the so-called apparent height) on the operating frequency *f*. A typical ionogram under calm

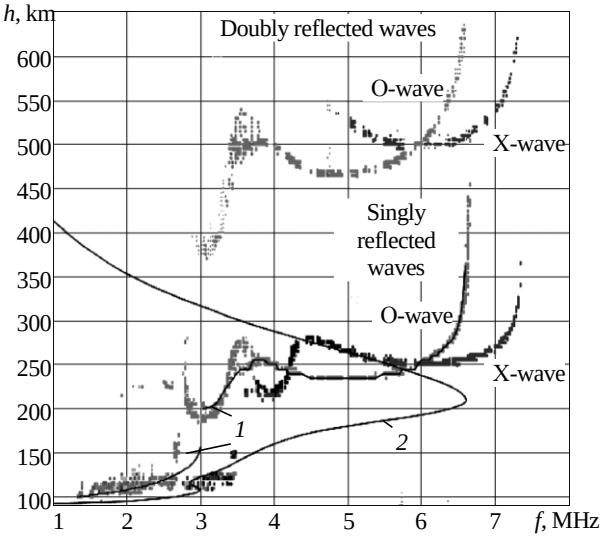


*Fig. 5*. Ionogram and calculated electron concentration profile under calm ionospheric conditions

ionospheric conditions is shown in Fig. 5. The received signal amplitude is depicted by the incremental darkening of the marks. Four signals parts are visible: singly reflected O- and X-waves; and doubly reflected O- and X-waves. When scattering in the ionosphere is practically absent the ionograms are clear traces under calm conditions (Fig. 5).

The signal of the singly reflected O-wave is usually used in calculations. The signal is traced by the programme (Fig. 5, *1*), and this trace is used to automatically calculate the electron density distribution over the ionosphere height (Fig. 5, *2*), namely the electron concentration profile.

The DPS-4 can operate as a classic radar with Doppler filtering of signals and determining the arrival angles of radio signals reflected from a target (ionosphere), in addition to frequency range scanning. In this mode, the DPS-4 cycles through several fixed frequency intervals. The measured amplitudes and phases of four antennas (Fig. 4) are stored in special DFT format files [12]. The results of processing these files are the arrival angles of radio waves (with a cells division by range and Doppler shift) and so-called sky maps (SM). They display the power distribution on the arrival angles of the radio waves reflected from the ionosphere with irregularities. Fig. 6 presents the sky map obtained from the data used to build the ionogram in Fig. 5. Fig. 6 shows that signals reflected from the ionosphere arrive from a very narrow cone of angles close to zenith (crosses indicate signals with a positive Doppler shift. The squares indicate signals with a negative

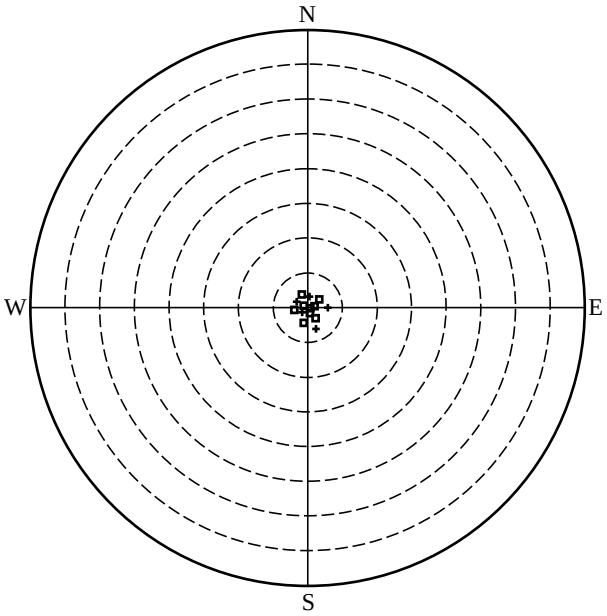


*Fig. 6*. Sky map constructed from the ionogram data (*Fig.5*)

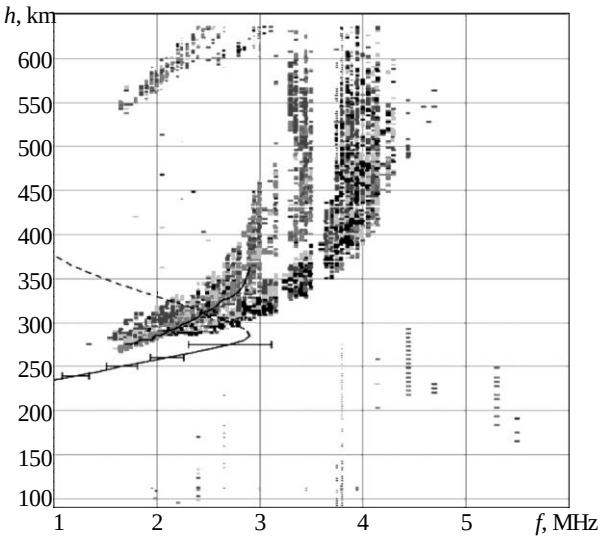


*Fig. 7*. Ionogram showing scattering on ionospheric irregularities (Moscow , 11.01.2014 00:25 UT)

Doppler shift). The power distribution obtained on the arrival angles is typical for calm ionospheric conditions when ionospheric irregularities are absent and, thus, there is no scattering on them.

Probe signals scattering is observed in the mid-latitude ionosphere for most of the time [6]. In this case, the ionogram traces expand in height and frequency. In this way the ionograms appear as shown in Fig. 7. The ionogram part depicted by the solid line is obtained as a result of direct measurements, and the part depicted by the dashed line is obtained by a computer simulation. In this case, the cone from

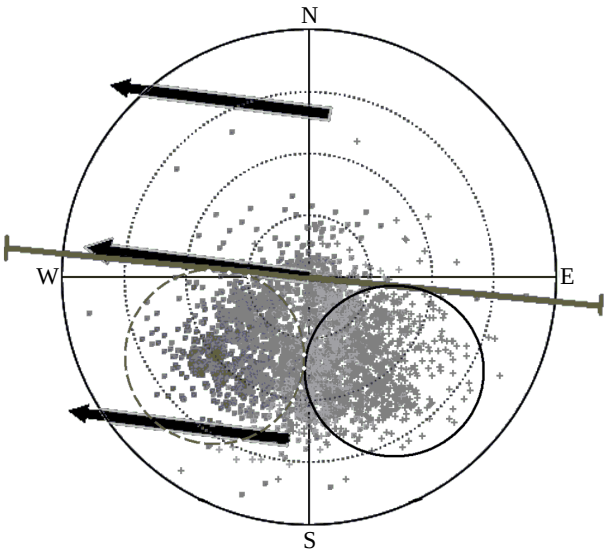


*Fig. 8*. Sky map under conditions of ionospheric scattering (Moscow , 11.01.2014 00:25 UT) (see Fig. *7*).

which scattered radio waves arrive to the earth expands, and its centre can significantly deviate from the zenith (Fig. 8). Moreover, the regions of maximum wave localisation with the positive (crosses; the region encircled by the solid line) and negative Doppler shift (squares; the region encircled by the dashed line) can vary. The following procedures can be performed by measuring the arrival angles and corresponding Doppler shifts for each reflector (ionosphere MSI), if at least three reflectors are present.

Considering that three selected reflectors have the same velocity vector, the system of equations is written, and all three components of this vector are found [11, 13, 15]. It is thus possible to obtain an array of vectors and estimate the mean and variance of the velocities by selecting various triples of reflectors. The averaging procedure can be carried out by considering weight coefficients which consider the relative power of various waves

A similar algorithm is used in the DPS-4 ionosonde software package. In standard mode, four fixed frequencies for probing procedure are automatically selected after the ionogram recording. Next, sky maps are constructed and the three components of the irregularities velocity are defined. The values obtained are displayed and stored in the array with the construction of daily charts.

Fig. 8 shows an automatically generated DPS-4 image (simplified). Original colour images of ionograms and sky maps can be found in [14]. The SM in Fig. 8 corresponds to the ionogram in Fig. 7. The arrows in Fig. 8

show the drift direction averaged over all reflectors from this region. The horizontal motion of irregularities occurs directionally from the region with predominantly positive Doppler frequency shifts toward the region with predominantly negative shifts (see arrows $v_{vert}$ in Fig. 1 and Fig. 8).

The accuracy of the velocity measurement depends on the scattering intensity. In the daytime, when lower ionospheric scattering is present (less irregularities on the sky map and the cone around the zenith is narrow), the accuracy of velocity measurement is often unsatisfactory. During the night, when there are hundreds or thousands of irregularities on the sky map, velocity measurement accuracy is higher, and the estimation of velocity dispersion used to determine measurement accuracy is sufficiently accurate. Measurements can be considered satisfactory if the mean velocity values are 3–5 times higher than the standard deviations.

Night-time measurements are used in the results presented below for comparisons.

**Experimental results.** The amplitude tomographic approach has been successfully applied in a number of works [10, 17–20]. The system of Russian satellites operating at frequencies of 150 and 400 MHz with almost circular orbits of about 1000 km was used. It is shown that cross-field anisotropy orientation $\psi_a$ correlates with the plasma drift direction $\psi_{dr}$

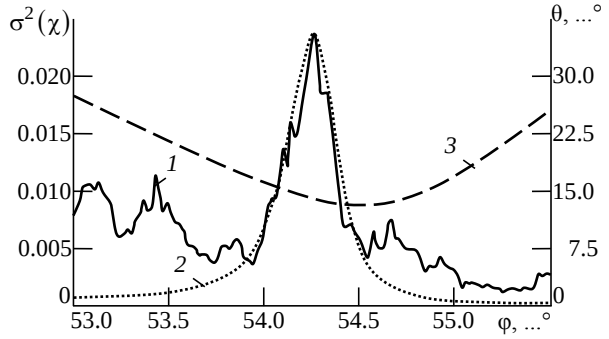


*Fig. 9*. The dependence between the logarithm dispersion of signal relative amplitude and angle between the magnetic field vector and line connecting the satellite with its latitude (Moscow, 15.01.2014 16:46 UT):
*1* – experiment; *2* – simulation; *3* – angle between the magnetic field vector and line connecting the satellite with its latitude

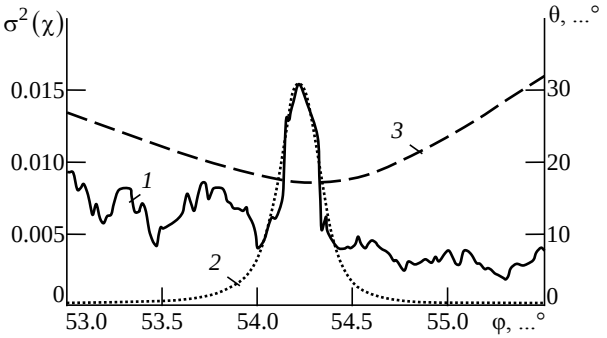


*Fig. 11*. The dependence between the logarithm dispersion of signal relative amplitude and angle between the magnetic field vector and line connecting the satellite with its latitude (Moscow, 26.01.2014 02:18 UT):
*1* – experiment; *2* – simulation; *3* – angle between the magnetic field vector and line connecting the satellite with its latitude

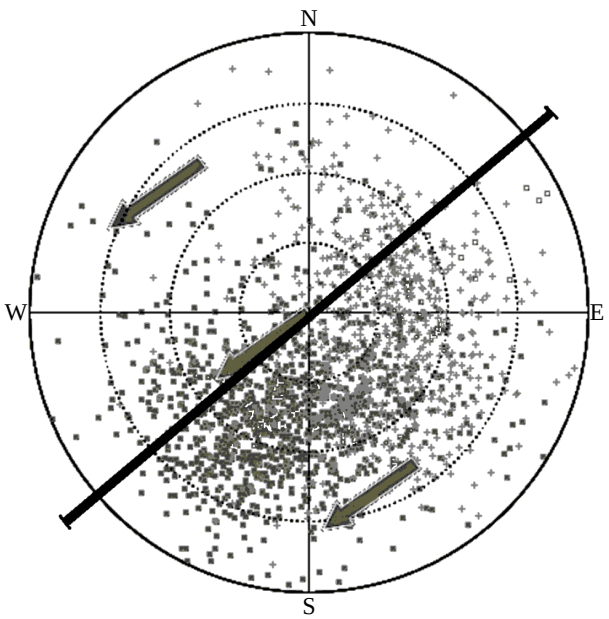


*Fig. 10*. Sky map under conditions of ionospheric scattering (Moscow, 15.01.2014 16:46 UT) (see Fig. *9*)

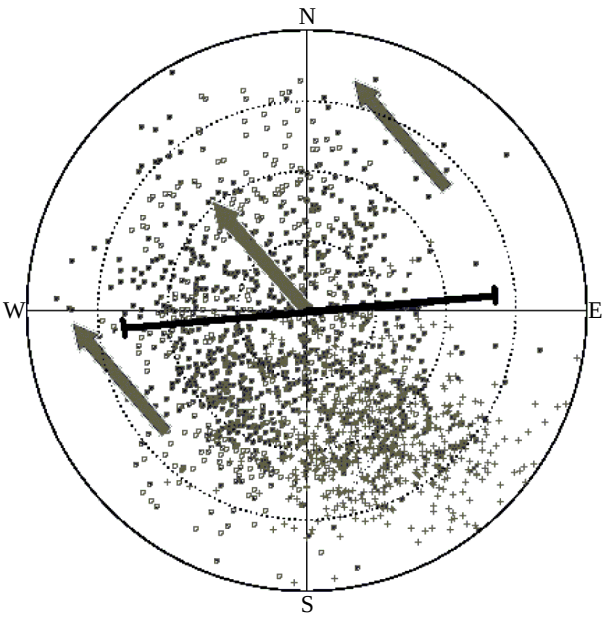


*Fig. 12*. Sky map under conditions of ionospheric scattering (Moscow, 26.01.2014 02:18 UT) (see Fig. *11*)

in the polar cap and auroral zone by using data from incoherent scattering radars and SuperDARN system. The elongation of high latitude irregularities along the geomagnetic field (α axis) varies from 10 to 100…150, and their elongation perpendicular to the geomagnetic field (β axis) varies from 3 to 30…40. This indicates the cross-field anisotropy of irregularities. The study of mid-latitude irregularities shows that they are also elongated mainly along the geomagnetic field in a certain direction perpendicular to it. The parameters α and β are numerically similar to the parameters of high latitude irregularities [21], while their cross-field anisotropy orientation $\psi_a$ varies under different geophysical conditions [21].

Previously there was an absence of plasma drift data in the midlatitude ionosphere in the European part of Russia due to the lack of incoherent scattering radars and SuperDARN systems. The $\psi_a$ orientation for midlatitudes were compared only with the neutral winds model [21]. The $\psi_a$ orientation can be compared with plasma drift experimental data obtained by the radar method in the Moscow region at the same time moments.

The data selected for comparison was the SSI orientations $\psi_a$ successfully defined by the reception centre data in Moscow. This is only possible in about 3% of the entire data array on the AS signals amplitude, since the applicability criterion for the method requires, firstly, the presence of a maximum in the logarithm dispersion graph of the relative amplitude, and, secondly, that the value of this maximum does not exceed 0.3. This is due to the fact that the calculations of the theoretical model of scattering on irregularities are performed within the framework of Rytov's approximation [16]. In January 2014, there were three successful sessions: on 11 January at 00:25 UT (Fig. 3, 7, 8), on 15 January at 16:46 UT (Fig. 9, 10) and on 26 January at 02:18 UT (Fig. 11, 12). The results of these measurements were compared with estimates of the velocity and plasma drift direction automatically obtained by the radar method by using the DPS-4 ionosonde located in ISMIRAN and operating in standard 15-minutes mode. The sky maps closest to the indicated moments in geographic coordinates were extracted from the archive for comparison with the directions of $\psi_a$ orientation. Fig. 8 presents data at 00:19 UT on January 11, 2014. The MSI drift direction $\psi_{dr}$=278° is indicated by arrows. In Fig. 8 the SSI orientation is shown by a segment $\psi_a$=95°≡275°, since the $\psi_a$ orientation is invariant to 180° rotation. In the session at 16:46 UT on 15 January the following parameters were obtained: $\alpha = 30$, $\beta = 7$, $\psi_a = 50^o \equiv 230^o$ and $\psi_{dr}$=235° (Fig. 9, 10).

On 11 January (Fig. 8) and 15 January (Fig. 10), the sky maps show good agreement between the cross-field anisotropy orientation $\psi_a$ and MSI drift direction $\psi_{dr}$ measured almost at the same time.

However, on 26 January a slightly different situation can be observed. Initially, the entire sky map was used for the $\psi_{dr}$ calculation (Fig. 11), as in the cases of January 11 and 15. The calculation was performed automatically by using the DriftExplorer associated with the DPS-4. The value $\psi_{dr}$=320° was obtained (arrows in Fig. 12). At the same time, the cross-field anisotropy orientation value in this session is $\psi_a = 85^o \equiv 265^o$ (Fig. 11 and the segment in Fig. 12). This discrepancy required further consideration.

As a result, G. N. Zhbankov developed a programme for determining drift direction by using sky maps. It is similar to the DriftExplorer, but more flexible in terms of settings. The programme thus developed calculated the identical orientation value $\psi_{dr}$=320° when processing the entire SM (Fig. 10). However, a much better agreement between the measured directions of $\psi_a$ and $\psi_{dr}$ was obtained when limiting the calculation region of reflections in Fig. 10 in terms of the region where the maximum amplitude fluctuations are observed. This is explained by the fact that the drift direction is now determined in the limited region as close as possible to the SSI spatial position [22].

**Conclusion.** The processing of the experimental logarithm dispersion curves of the relative signal amplitude during the satellite passing showed that the irregularities have cross-field anisotropy in the F region at midlatitudes, as well as at high latitudes, since not a single maximum can be approximated when β = 1 by the model of isotropic elongated irregularities. Small-scale irregularities in the midlatitude ionosphere tend to elongate in the cross-field direction close to the direction of the MSI drift. More accurate data, and more specific case features will lead to an improvement in data agreement. The correlation revealed between the cross-field anisotropy orientation of the elongated irregularities and their drift direction can be useful when there is a lack of information on ionospheric irregularities.

## References

1. Bryunelli B. E., Namgaladze A. A. *Fizika ionosfery* [Ionosphere Physics]. Moscow, *Nauka*, 1988, 526 p. (In Russ.)

2. Al'pert Ya. L. *Rasprostranenie elektromagnitnykh voln i ionosfera* [Propagation of Electromagnetic Waves and Ionosphere]. 2nd ed. Moscow, *Nauka*, 1972, 564 p. (In Russ.)

3. International Reference Ionosphere. Available at: http://irimodel.org (accessed 21.07.2019)

4. Shubin V. N., Karpachev A. T., Telegin V. A., Tsybulya K. G. SMF2 Global Model of F2 Layer Peak Maximum From Satellite and Ground-Based Observation. Available at: http://smf2.izmiran.ru (accessed 21.07.2019)

5. Gershman B. N., Kazimirovskii E. S., Kokourov V. D., Chernobrovkina N. A. Yavlenie F-rasseyaniya v ionosfere [The F-Scattering Phenomenon in the Ionosphere]. Moscow, *Nauka*, 1984, 140 p. (In Russ.)

6. Panchenko V. A., Telegin V. A., Vorob'ev V. G., Zhbankov G. A., Yagodkina O. I., Rozhdestvenskaya V. I. Spread F in the Midlatitude Ionosphere According to DPS-4 Ionosonde Data. Geomagnetizm i Aeronomiya. 2018, vol. 58, no. 2, pp. 241–249.

7. Yasyukevich Yu. V., Zhivet'ev I. V., Yasyukevich A. S., Voeikov S. V., Zakharov V. I., Perevalova N. P., Titkov N. N. Influence of Ionospheric and Magnetospheric Disturbances on Failures of Global Navigation Satellite Systems. Current Problems in Remote Sensing of the Earth from Space. 2017, vol. 14, no. 1, pp. 88–98. (In Russ.)

8. Nasyrov A. M. *Rasseyanie radiovoln anizotropnymi ionosfernymi neodnorodnostyami* [Radio Wave Scattering by Anisotropic Ionospheric Inhomogeneities]. Kazan, *Izdvo Kazanskogo un-ta*, 1991, 150 p. (In Russ.)

9. Sergeev E. N., Zykov E. Yu., Akchurin A. D., Nasyrov I. A., Vertogradov G. G., Vertogradov V. G., Kim V. Yu., Polimatidi V. P., Grach S. M. The Results of Comprehensive Studies of the Perturbed Region of the Ionosphere Using a Short-Wavelength Location in a Wide Frequency Band and Artificial Radiation of the Ionosphere. Radiophysics and Quantum Electronics. 2012, vol. 55, no. 1/2, pp. 79–93. (In Russ.)

10. Tereshchenko E. D., Khudukon B. Z., Kozlova M. O., Nygren T. Anisotropy of Ionospheric Irregularities Determined from the Amplitude of Satellite Signals at a Single Receiver. Ann. Geophysicae. 1999, vol. 17, pp. 508–518.

11. Livingston R. S., Rino C. L., Owen J., Tsunoda R. T. The Anisotropy of High-Latitude Nighttime F Region Irregularities. J. Geophys. Res. 1982, vol. 87, no. 12, pp. 10519–10526.

12. Digisonde4DManual_LDI-web1-2-6. Technical Manual. Ver. 1.2.6. Available at: http://digisonde.com/dps-4dmanual.html (accessed 21.07.2019)

13. Reinisch B. W., Galkin I. A., Khmyrov G. M., Kozlov A. V., Bibl K., Lisysyan I. A., Cheney G. P., Huang X., Kitrosser D. F., Paznukhov V. V., Luo Y., Jones W., Stelmash S., Hamel R., Grochmal J. The New Digisonde for Research and Monitoring Applications. Radio Sci. 2009, vol. 44, iss. 1. doi: 10.1029/2008RS004115

14. Available at: http://147.231.47.3 (accessed 21.07.2019)

15. Galushko V. G., Kascheev A. S., Paznukhov V. V., Yampolski Yu. M., Reinisch B. W. Frequency-and-Angular Sounding of Traveling Ionospheric Disturbances in the Model of Three-Dimensional Electron Density Waves. Radio Sci. 2008, vol. 43, iss. 4. doi: 10.1029/2007RS003735

16. Rytov S. M., Kravtsov Yu. A., Tatarskii V. I. *Vvedenie v statisticheskuyu radiofiziku. Ch. 2. Sluchainye polya* [Introduction to Statistical Radiophysics. Part 2. Random Fields.]. Moscow, *Nauka*, 1978, 463 p. (In Russ.)

17. Tereshchenko E. D., Khudukon B. Z., Kozlova M. O., Evstafiev O. V., Nygren T., Brekke A. Comparison of the Orientation of Small Scale Electron Density Irregularities And F Region Plasma Flow Direction. Ann. Geophysicae. 2000, vol. 18, no. 8, pp. 918–926.

18. Tereshchenko E. D., Khudukon B. Z., Kozlova M. O., Evstafiev O. V., Nygren T. Anisotropy of Ionospheric Irregularities Determined from the Amplitude of Satellite Signals at a Singlereciver. Ann. Geophysicae. 1999, vol. 17, no. 4, pp. 508–518.

19. Tereshchenko E. D., Romanova N. Yu., Koustov A. V. VHF Scintillations, Orientation of the Anisotropy of F-region Irregularities and Direction of Plasma Convection in the Polar Cap. Annales Geophysicae. 2008, vol. 26, iss. 7, pp. 1725–1730. doi: 10.5194/angeo-26-1725-2008

20. Tereshchenko E. D., Romanova N. Yu., Kustov A. V. Comparison of Transverse to Magnetic Field Anisotropy of Small-Scale Inhomogeneities with Ionospheric Convection According to SuperDARN Radars. Geomagnetism and Aeronomy. 2004, vol. 44, no. 4, pp. 487–492. (In Russ.)

21. Romanova N. Yu. The Relationship Between the Direction of the Horizontal Wind and the Orientation of the Transverse Anisotropy of Small-Scale Inhomogeneities in the F Region of the Mid-Latitude Ionosphere. Geomagnetism and Aeronomy. 2017, vol. 57, no. 4, pp. 463–471.

22. Telegin V. A., Romanova N. Yu., Panchenko V. A., Zhbankov G. N. *Ob orientatsii poperechnoi anizotropii melkomasshtabnykh neodnorodnostei F-oblasti v napravlenii dreifa nad Moskvoi v yanvare 2014 goda* [On the Orientation of the Transverse Anisotropy of Small-Scale Inhomogeneities of the F-Region in the Direction of Drift over Moscow in January 2014]. Physics of Auroral Phenomena, Abstracts of 42nd Annual Seminar 11–15 March, 2019, Apatity, p. 58. (In Russ.)

## Information about the authors

**Valery A. Panchenko,** Cand. Sci. (Phys.) (1993), Senior Scientist in Pushkov Institute of Terrestrial Magnetism, Ionosphere and Radio Wave Propagation Russian Academy of Sciences. The author of more than 80 scientific publications. Area of expertise: Doppler and other radio methods of the irregular structure of the ionosphere investigations.
E-mail: panch@izmiran.ru
https://orcid.org/0000-0003-2870-618X

**Viktor A. Telegin**, Dr. Sci. (Phys.) (1984), Head of Laboratory in Pushkov Institute of Terrestrial Magnetism, Ionosphere and Radio Wave Propagation Russian Academy of Sciences. The author of more than 100 scientific publications. Area of expertise: investigation of ionospheric irregularities by vertical and external sounding methods.
E-mail: telegin@izmiran.ru
https://orcid.org/0000-0002-1837-6335

**Natalia Yu. Romanova**, Researcher at the Polar Geophysical Institute KSC RAS. The author of 20 scientific publications Area of expertise: structure of a high- and middle-latitude ionosphere, ionosphere of polar cap.
E-mail: romanova@pgi.ru
https://orcid.org/0000-0001-6867-4851

## Список литературы

1. Брюнелли Б. Е., Намгаладзе А. А. Физика ионосферы. М.: Наука, 1988. 526 с.

2. Альперт Я. Л. Распространение электромагнитных волн и ионосфера. 2-е изд. М.: Наука, 1972. 564 с.

3. International Reference Ionosphere. URL: http://irimodel.org (дата обращения: 21.07.2019)

4. SMF2 Global Model of F2 Layer Peak Maximum From Satellite and Ground-Based Observation / V. N. Shubin, A. T. Karpachev, V. A. Telegin, K. G. Tsybulya. URL: http://smf2.izmiran.ru (дата обращения: 21.07.2019)

5. Явление F-рассеяния в ионосфере / Б. Н. Гершман, Э. С. Казимировский, В. Д. Кокоуров, Н. А. Чернобровкина. М: Наука, 1984. 140 с.

6. Spread F in the Midlatitude Ionosphere According to DPS-4 Ionosonde Data / V. A. Panchenko, V. A. Telegin, V. G. Vorob'ev, G. A. Zhbankov, O. I. Yagodkina, V. I. Rozhdestvenskaya // Geomagnetizm i Aeronomiya. 2018. Vol. 58, № 2. P. 241–249.

7. Влияние ионосферной и магнитосферной возмущенности на сбои глобальных навигационных спутниковых систем / Ю. В. Ясюкевич, И. В. Живетьев, А. С. Ясюкевич, С. В. Воейков, В. И. Захаров, Н. П. Перевалова, Н. Н. Титков // Соврем. проблемы дистанционного зондирования Земли из космоса. 2017. Т. 14, № 1. С. 88–98.

8. Насыров А. М. Рассеяние радиоволн анизотропными ионосферными неоднородностями. Казань: Изд-во Казан. ун-та, 1991. 150 с.

9. Результаты комплексных исследований возмущенной области ионосферы с помощью коротковолновой локации в широкой полосе частот и искусственного излучения ионосферы / Е. Н. Сергеев, Е. Ю. Зыков, А. Д. Акчурин, И. А. Насыров, Г. Г. Вертоградов, В. Г. Вертоградов, В. Ю. Ким, В. П. Полиматиди, С. М. Грач // Изв. вузов. Радиофизика. 2012. Т. 55, № 1/2. С. 79–93.

10. Anisotropy of Ionospheric Irregularities Determined from the Amplitude of Satellite Signals at a Single Receiver / E. D. Tereshchenko, B. Z. Khudukon, M. O. Kozlova, T. Nygren // Ann. Geophysicae. 1999. Vol. 17. P. 508–518.

11. The Anisotropy of High-Latitude Nighttime F Region Irregularities / R. S. Livingston, C. L. Rino, J. Owen, R. T. Tsunoda // J. Geophys. Res. 1982. Vol. 87, № 12. P. 10519–10526.

12. Digisonde4DManual_LDI-web1-2-6. Technical Manual. Ver. 1.2.6. URL: http://digisonde.com/dps-4dmanual.html (дата обращения: 21.07.2019)

13. The New Digisonde for Research and Monitoring Applications / B. W. Reinisch, I. A. Galkin, G. M. Khmyrov, A. V. Kozlov, K. Bibl, I. A. Lisysyan, G. P. Cheney, X. Huang, D. F. Kitrosser, V. V. Paznukhov, Y. Luo, W. Jones, S. Stelmash, R. Hamel, J. Grochmal // Radio Sci. 2009. Vol. 44, iss. 1. doi: 10.1029/2008RS004115

14. URL: http://147.231.47.3 (дата обращения: 21.07.2019)

15. Frequency-and-Angular Sounding of Traveling Ionospheric Disturbances in the Model of Three-Dimensional Electron Density Waves / V. G. Galushko, A. S. Kascheev, V. V. Paznukhov, Yu. M. Yampolski, B. W. Reinisch // Radio Sci. 2008. Vol. 43, iss. 4. doi: 10.1029/2007RS003735

16. Рытов С. М., Кравцов Ю. А., Татарский В. И. Введение в статистическую радиофизику. Ч. 2: Случайные поля. М.: Наука, 1978, 463 с.

17. Comparison of the Orientation of Small Scale Electron Density Irregularities And F Region Plasma Flow Direction / E. D. Tereshchenko, B. Z. Khudukon, M. O. Kozlova, O. V. Evstafiev, T. Nygren, A. Brekke // Ann. Geophysicae. 2000. Vol. 18, № 8. P. 918–926.

18. Anisotropy of Ionospheric Irregularities Determined from the Amplitude of Satellite Signals at a Singlereciver / E. D. Tereshchenko, B. Z. Khudukon, M. O. Kozlova, O. V. Evstafiev, T. Nygren // Ann. Geophysicae. 1999. Vol. 17, № 4. P. 508–518.

19. Tereshchenko E. D., Romanova N. Yu., Koustov A. V. VHF Scintillations, Orientation of the Anisotropy of F-region Irregularities and Direction of Plasma Convection in the Polar Cap // Annales Geophysicae. 2008. Vol. 26, iss. 7. P. 1725–1730. doi: 10.5194/angeo-26-1725-2008

20. Терещенко Е. Д., Романова Н. Ю., Кустов А. В. Сопоставление поперечной к магнитному полю анизотропии мелкомасштабных неоднородностей с ионосферной конвекцией по данным радаров SuperDARN // Геомагнетизм и аэрономия. 2004. Т. 44, № 4. С. 487–492.

21. Романова Н. Ю. Взаимосвязь между направлением горизонтального ветра и ориентацией поперечной анизотропии мелкомасштабных неоднородностей в F-области среднеширотной ионосферы // Геомагнетизм и аэрономия. 2017. Т. 57, № 4. С. 463–471.

22. Об ориентации поперечной анизотропии мелкомасштабных неоднородностей F-области в направлении дрейфа над Москвой в январе 2014 года / В. А. Телегин, Н. Ю. Романова, В. А. Панченко, Г. Н. Жбанков // Physics of Auroral Phenomena, Abstracts of 42nd Annual Seminar, Апатиты, 11–15 March, 2019. P. 58.

## Информация об авторах

**Панченко Валерий Алексеевич** – кандидат физико-математических наук (1993), старший научный сотрудник ИЗМИРАН. Автор более 80 научных публикаций. Сфера интересов – доплеровский и другие радиометоды в исследовании неоднородной структуры ионосферы.
E-mail: panch@izmiran.ru
https://orcid.org/0000-0003-2870-618X

**Телегин Виктор Алексеевич** – кандидат физико-математических наук (1984), заведующий лабораторией в ИЗМИРАН. Автор более 100 научных публикаций. Сфера интересов – исследование ионосферных неоднородностей методами вертикального и внешнего зондирования.
E-mail: telegin@izmiran.ru
https://orcid.org/0000-0002-1837-6335

**Романова Наталья Юрьевна** – дипломированный специалист по специальности "Учитель физики и общетехнических дисциплин" (1999, Мурманский государственный педагогический университет), младший научный сотрудник Полярного геофизического института КНЦ РАН. Автор 20 научных публикаций. Сфера интересов – структура полярной и среднеширотной ионосферы, ионосферы в полярной шапке.
E-mail: romanova@pgi.ru
https://orcid.org/0000-0001-6867-4851